ISSN 0036-0236, Russian Journal of Inorganic Chemistry, 2022, Vol. 67, No. 3, pp. 338–349. © Pleiades Publishing, Ltd., 2022.
Russian Text © The Author(s), 2022, published in Zhurnal Neorganicheskoi Khimii, 2022, Vol. 67, No. 3, pp. 360–372.

COORDINATION COMPOUNDS

Generation and Spectral Properties of Oxidized Forms of Iridium and Rhenium Porphyrin Complexes

E. Yu. Tyulyaeva[a], *, N. G. Bichan[a], and T. N. Lomova[a]

[a] *Krestov Institute of Solution Chemistry, Russian Academy of Sciences, Ivanovo, 153045 Russia*

**e-mail: teu@isc-ras.ru*

Received September 7, 2021; revised September 14, 2021; accepted September 20, 2021

Abstract—We make a brief overview of the results of studies into the reactivity of iridium and rhenium complexes in various oxidation states with substituted, expanded, *N*-fused, and *N*-confused porphyrins, corroles, as well as heteroatomic macrocycles under chemical and electrochemical oxidation conditions. The characteristic spectral features of the species are analyzed, as well as the key factors responsible for the stabilization of the charge of the complexing ion and the charge location during the oxidation of compounds on the aromatic part of the molecule, the central metal atom, or the axial ligand. Iridium and rhenium in the oxidation state of +1 to +7 form stable complexes with porphyrins and their analogues, which are of particular interest due to their unusual properties and a potential for use in various fields of science and technology, including advanced materials and catalysts. The high reactivity in redox processes with a reaction center on the macrocycle or on the central ion is the main feature of iridium and rhenium porphyrin complexes. The high stability not only of molecular species, but also of charged radical species of complexes is of great interest for further progress in the study of the mechanisms of their chemical and photophysical transformations, understanding of which is necessary for the development of applied chemistry of porphyrin complexes of iridium, rhenium, and their analogues.

Keywords: iridium, rhenium, porphyrin complexes, oxidation, radical cations

DOI: 10.1134/S0036023622030147

INTRODUCTION

Iridium and rhenium are among the rarest elements due to their negligible natural abundance. However, the variety of formal oxidation states (from +1 to +5 in Ir, from +1 to +7 in Re), combined with the ability of aromatic tetrapyrrole ligands to stabilize unusual metal oxidation states, provides porphyrin complexes of iridium (IrP) and rhenium (ReP) with unique properties promising for use in radiopharmacology in diagnosing and treating diseases and in the design and use of luminescent materials and catalysts [1–10]. It is due to the combination of rich redox properties and coordination unsaturation that tetrapyrrole complexes of iridium and rhenium are considered suitable synthetic models for studying one-electron and two-electron oxidative processes during oxygen transfer in catalytic cycles of natural enzymes, along with complexes such as iron and manganese porphyrins [11–14]. The prospects of using IrP and ReP as catalysts for reactions of organic compounds [15–30], water oxidation [31, 32], and oxygen reduction [33] are also discussed. Evidence has been published for the use of those complexes as electron donors in systems with photoinduced electron transport, where their short-lived radical-cation forms are realized [34–37], and as biocompatible and biodegradable oxygen probes [38].

THEORETICAL PART

The subject matter of this work is the generalization and analysis of the related literature and our own data on the preparation and properties of oxidized forms, including radical species, of iridium and rhenium complexes in various oxidation states with substituted, expanded, *N*-fused, *N*-confused porphyrins, corroles, as well as heteroatomic macrocycles. The specificity of properties of oxidized and radical species of IrP and ReP complexes dictates the applicability of certain physical and physicochemical methods in their characterization. The electronic absorption spectra (EAS) of oxidized IrP and ReP forms are of the same type for the reasons described in the next section, and are quite characteristic (Fig. 1).

Electronic paramagnetic resonance (EPR) is informative only for a certain distribution of the unpaired electron spin over the atoms of the macrocycle, and is inapplicable to weak bonding between radical and metal centers [39]. Therefore, UV–Vis spectroscopy was recognized as the best method in the early stages of research for the characterization of radical species

of metalloporphyrins [40, 41]. While the electronic absorption spectrum still remains the simplest tool for identifying π-radical cations, the combined use of XRD, EPR, NMR spectroscopy, and quantum-chemical calculations at present makes it possible to characterize unpaired electron spin density distribution in more complex systems. The results of EPR studies and DFT (B3LYP/6-311G(d,p)) calculations were used to determine the unpaired electron spin distribution over the atoms of the diazaporphyrin ring in 3*d*-metal complexes [42–44]. In addition, ferromagnetic spin coupling is observed between the paramagnetic central ion (Cu^{II}) and π radical [45]. The availability of the quantitative energy characteristics of the boundary MOs of $Co^{II}P^{\bullet+}$ and $Mn^{III}P^{\bullet+}$ π-radical-cations in photoinduced radical salts with a fullerene-containing radical-anion was shown by DFT and TD-DFT (B3LYP* + D3BJ/6-31G level) quantum-chemical calculations and by femtosecond transient absorption spectroscopy [46].

Formation of oxidized MP species is manifested in IR spectra. For one-electron-oxidized macrocyclic species, bands are observed due to the vibrations of C_α–C_β and C_α–N bonds in pyrrole rings in the range 1300–1600 cm^{-1}. The most noticeable of them, confirming the porphyrin type, rather than the symmetry state, are the bands at ~1280 cm^{-1}, corresponding to π-radical cation complexes of H_2TPP, and the bands at ~1550 cm^{-1}, typical of $MOEP^{\bullet+}$ [47]. However, the presence of axial and peripheral substituents and their nature (in particular, in *meso*-phenyls) significantly affect the value of the frequency shift of the indicated types of vibrations in oxidized complex species [48]. The transition to two-electron-oxidized radical-dication species of dimeric complexes is accompanied by an increase in signal intensity with a slight shift [49, 50].

For porphyrin complexes of low-charge metal ions (Zn, Cu, Ni, Co, Mg, Fe, and Ru), the structures (distortion and bond lengths) of π-radical cations were studied by X-ray structural analysis and DFT calculations [51–55]. According to the calculations, the ring bond lengths change compared to a neutral molecule when aromatically oxidized tetrapyrrole molecules (porphyrins and phthalocyanines) are formed. The formation of radical-cation species brings about an increase in the difference between the bond lengths of alternating bonds in the porphyrin ring and in the angles between them, as opposed to delocalized bonds in the neutral molecule. Table 1 shows how the dihedral angles (ψ, deg.) between the planes of the porphyrin ring and *meso*-phenyl substituents change depending on the oxidation state of the molecule exemplified by ZnTPP and its phenyl-substituted analogues. Structural alterations enhance electron transfer among the neutral, radical-cation, and dication species.

However, there is difference between the results of theoretical calculations and X-ray structural analysis,

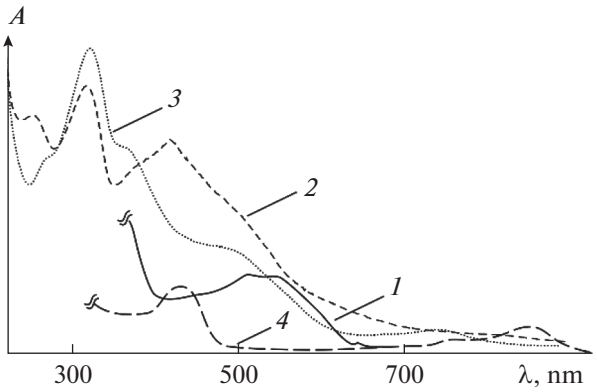

Fig. 1. Electronic absorption spectra of oxidized metalloporphyrin species: (*1*) $ClMnTPP^{+\bullet}$ in 2.52 M H_2O_2; (*2*) $(HSO_4)RhTPP^{+\bullet}$ in 17.41 M H_2SO_4; (*3*) $O{=}Re(HSO_4)MPOEP^{\bullet+}$ in 17.77 M H_2SO_4; and (*4*) $(CH_3COO)(CH_3COOH)IrTPP^{\bullet+}$ in 100% AcOH (TPP and OEP, respectively, stand for the 5,10,15,20-tetraphenyl-21*H*,23*H*-porphyrin dianion and 2,3,7,8,12,13,17,18-octaethyl-21*H*,23*H*-porphyrin dianion).

arising from the Jahn–Teller effect, according to which the interrelation of degenerate electronic states with distortions leads to the removal of degeneracy and a decrease in symmetry. Experimental data demonstrates the importance of environmental effects, which

Table 1. Values of dihedral angles (ψ, deg) between the porphyrin ring plane and the planes of *meso*-phenyl substituents in various degrees of oxidation as obtained by DFT (B3LYP 6-31G(d,p)) calculations [51]

Complex	Ψ*	Ψ**
ZnTPP	66.01	65.43
ZnT(2'-thienyl)P	65.26	63.57
ZnT(3'-furyl)P	58.37	57.13
ZnT(3'-thienyl)P	61.86	61.18
$ZnTPP^{\bullet+}$	55.86	56.00
$ZnT(2'\text{-thienyl})P^{\bullet+}$	44.78	44.74
$ZnT(3'\text{-furyl})P^{\bullet+}$	44.52	44.20
$ZnT(3'\text{-thienyl})P^{\bullet+}$	49.12	49.04
$ZnTPP^{2+}$	45.36	55.09
$ZnT(2'\text{-thienyl})P^{2+}$	34.46	34.46
$ZnT(3'\text{-furyl})P^{2+}$	35.53	34.61
$ZnT(3'\text{-thienyl})P^{2+}$	39.24	39.32

* Optimized for isolated molecules and radicals.

** Optimized in dichloromethane.ZnTPP = (5,10,15,20-tetraphenyl-21*H*,23*H*-porphinato)zinc(II), ZnT(2'-thienyl)P = (5,10,15,20-(2'-thienyl)-21*H*,23*H*-porphinato)zinc(II), ZnT(3'-furyl)P = (5,10,15,20-(3'-furyl)-21*H*,23*H*-porphinato)zinc(II), and ZnT(3'-thienyl)P = (5,10,15,20-(3'-thienyl)-21*H*,23*H*-porphinato)zinc(II).

are neither taken into account nor revealed in some calculations [52].

Cyclic voltammetry was used to determine the redox potentials of $Co^{II}Pc^{\bullet+}/Co^{II}Pc$ and $Mn^{III}Pc^{\bullet+}/Mn^{III}Pc$ (Pc stands for the phthalocyanine dianion) in 0.1 M $(n\text{-}Bu)_4NClO_4$ solution in dichloromethane, which were equal to 0.94 and 1.25 V, respectively, when complexes entered a donor–acceptor pair with axially coordinated 1'-*N*-methyl-2'-(1*H*-imidazol-1-yl)-phenylpyrrolidino[3',4':1,2][60]fullerene (ImC_{60}) [46]. The $Mn^{III}Pc$ fluorescence quenching effect (λ_{exs} = 365 nm) was also shown therein in the radical salt $Mn^{III}Pc^{\bullet+}/ImC_{60}^{\bullet-}$.

A comprehensive study of the effects of charge delocalization, oxidation state, and spin state of the central metal in highly oxidized species on ^1H NMR and EPR spectra is documented for iron porphyrin complexes [55].

RESULTS AND DISCUSSION

To predict the catalytic properties of compounds and elucidate the mechanism of catalysis on metalloporphyrins (MPs), it is important to know the properties of oxidized and reduced forms of the catalyst, which are intermediates of redox processes. The oxidation stability of MPs is mainly determined by the electronic nature of the complex-forming cation, macrocycle, its functional substituents, and ligands in the axial position. Many oxidized cationic and radical-cationic forms of IrP and ReP are observed in chemical, electrochemical, or photophysical transformations as relatively stable or short-lived. The removal of an electron during the electrochemical or chemical exposure of MRs can occur at the central atom or at the aromatic part of the molecule, and it can be accompanied either by an increase in the oxidation state of the complexing cation in the complex, or by the formation of a π-radical cation form of $MP^{\bullet+}$ molecules with the positive charge located on the macrocycle. Two types of π-radical cations of metalloporphyrins are distinguished depending on the unpaired electron spin distribution, namely: a $^2A_{1u}$ radical with the spin density on the C_{meso} atoms of methine bridges and intracyclic N atoms, and a $^2A_{2u}$ radical distinguished by a low spin density in *meso* positions [40, 41]. Since the electronic properties of these forms are similar, the symmetry of the state can be changed by replacing the axial ligand in the complex. Both types of the π-radical cations have similar electronic absorption spectra due to the closeness of the HOMO energies; this is the reason for the specificity of the EAS of metalloporphyrin π-radical cations. The degeneracy of two boundary orbitals (HOMO), which is typical of the initial molecules, is released both in the case of one-electron reduction of ZnTPP and in the case of one-electron oxidation of ZnPc, as shown by the ZINDO calculations of ZnPc and ZnTPP molecules, cations, and anions in terms of a 16-orbital model and magnetic dichroism data published in the fundamental work [56]. This catastrophically changes the EAS of the aforementioned compounds. In the ZnTPP spectrum, absorption bands with λ_{max} = 538 and 910 nm appear due to $\pi^* \rightarrow \pi^*$ transitions within vacant MOs. Simultaneously, the (0,0) and (0,1) Q bands lying at 605 and 560 nm in the parent ZnTPP spectrum, shift bathochromically by 145 and 168 nm, respectively. When one electron is removed (in going from ZnPc to $ZnPc^+$), similar new bands refer to the $\pi \rightarrow \pi$ transition inside the filled shells. Along with them, bathochromically shifted Q bands appear at 958 and 925 nm, the second $\pi \rightarrow \pi^*$ transition band appears at 300–450 nm, and B_1, B_2, and $\pi \rightarrow \pi^*$ bands appear. The overall result is a sharp increase in absorption at the border between the UV and the visible, the appearance of new bands in the near-infrared region, and a relative decay in adsorption at the site of the original Q bands, which is observed in the spectra of other one-electron-oxidized metalloporphyrins shown in Fig. 1. The appearance or non-appearance of MP absorption bands in the region 550–700 nm serves as the base for interpreting the available experimental data in order to identify macrocycle-oxidized compounds.

The generation of oxidized forms of iridium and rhenium tetrapyrrole compounds in electrochemical experiments is documented; however, it is not in every work that the oxidation processes are identified and the positive charge locality is indicated. For porphyrin Ir^{3+} complexes with various axial ligands and *meso*-phenyl and/or β-alkyl substituents in the macrocycle, the first oxidation potential assigned to the formation of a π-radical cation, is determined as 0.51–1.31 V [2, 57]. Doubly oxidized species are formed at 1.15–1.45 V; for H_2TPP complexes, the occurrence or nonoccurrence of this process depends on the nature of axial ligands. Studies of iridium(III) complexes with allied porphyrin analogues, namely, tripentafluoro- and tripara-X-phenylcorroles (X = CF_3, H, Me, or OMe (Fig. 2, structure **1**) indicate the oxidation of the central cation to Ir^{4+} at E = 0.20–1.69 V and a possibility of second oxidation to occur both at the macrocycle and at the iridium cation at E = 0.89–1.18 V [3, 58].

$Ir(C_8H_{13})OEP$ and $Ir(C_8H_{13})(CO)OEP$, which are iridium complexes axially coordinated by alkyl groups, are the first examples of metalloporphyrins σ-bonded along the axial axis that can be reversibly oxidized at the axial ligand in tetrahydrofuran at 0.68 and 0.80 V, respectively [59]. Oxidation of the axial part of a molecule was also observed in the reaction of $(CH_2COAr)IrTTP$ (TTP is 5,10,15,20-tetratholyl-21H,23H-porphine dianion) with 1-oxy-2,2,6,6-tetramethylpiperidinyl, where the suggested intermediate with the radical located on a carbon atom $Ir^{III}(CH_2CHR^{\bullet})$ was stabilized by the central cation and the reaction product was the com-

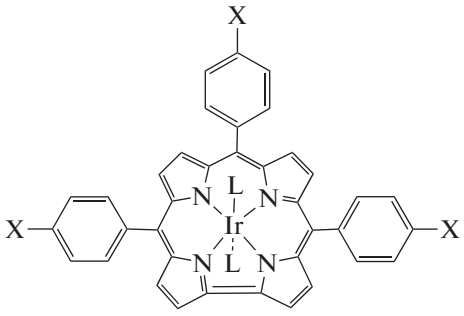

$X = CF_3$, H, CH_3, OCH_3

Structure **1**

Fig. 2. Chemical structure of triphenylcorroles. L = pyridine (py), trimethylamine (tma), isoquinoline (isoq), 4-dimethylaminopyridine (dmap), and 4-picolinic acid (4pa).

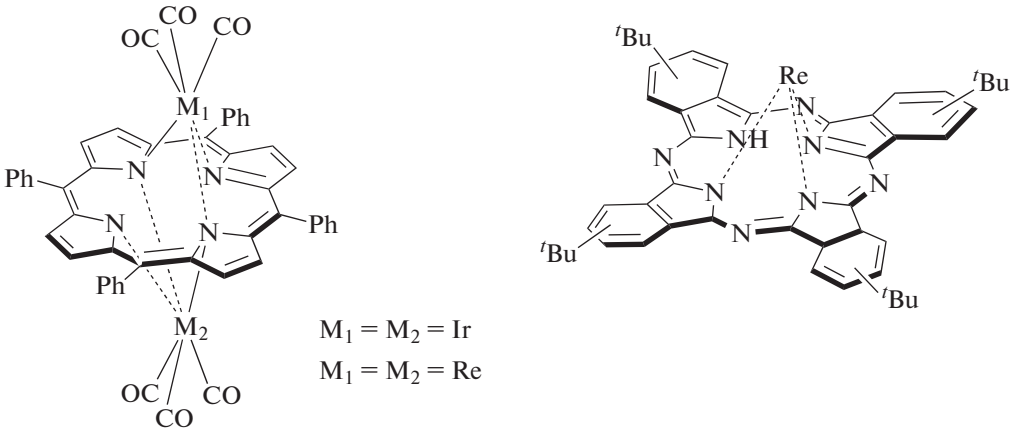

2 **3**

Structures **2** and **3**

Fig. 3. Chemical structure of binuclear iridium(I) and rhenium(I) complexes with H_2TPP (structure **2**) and mononuclear rhenium(I) complex with substituted H_2Pc (structure **3**).

plex $Ir^{II}(CH_2{=}CHR)$ with the unpaired electron on the metal [60].

The binuclear iridium(I) complex $(TPP)[Ir^{I}(CO)_3]_2$ (Fig. 3, structure **2**) has two oxidation potentials: 0.92 and 1.5 V in benzonitrile (PhCN) or CH_2Cl_2 containing 0.2 M tetrabutylammonium perchlorate [61]. $[(TPP)Ir^{III}]^{+}ClO_4^{-}$ is produced by the first (rapid and irreversible) electrooxidation of the metal ($Ir^{I} \rightarrow Ir^{III}$) with CO cleavage detected by the disappearance of the vibration bands due to Ir–CO bonds at 2054 and 1979 cm^{-1} from the IR spectrum of the initial compound. Further, an electron is removed from the macrocycle at 1.5 V in the same way as in other iridium(III) porphyrin complexes.

In isostructural rhenium(I) complexes $(TPP)[Re^{I}(CO)_3]_2$ (Fig. 3, structure **2**) and $(^{t}BuPc)[Re^{I}(CO)_3]_2$, unlike in $(TPP)[Ir^{I}(CO)_3]_2$, the metal oxidation state does not change under electrochemical exposure. The observed spectral evolution and changes in E_{ox} are typical of species oxidized at the macrocycle: 1.01 V (CH_2Cl_2), 1.16 V (PhCN) for the porphyrin complex [62] and 0.52 V for the phthalocyanine complex [63]. The mononuclear complex $(^{t}BuPc)Re^{I}(CO)_3$ (Fig. 3, structure **3**) undergoes oxidation two times, at 0.32 and 0.76 V; however, the first electron release process is not assigned in the cited work [63].

The oxidation potentials of substituted *N*-confused-porphyrin (NCP) complexes of rhenium(I) and rhenium(V), which appear on Scheme 1, vary in the range 0.1–0.6 V depending on the oxidation number of the central atom and the extent of the π-electron system. Significant bathochromic shifts in

the EASs of chemically oxidized species and the lower magnitudes of oxidation potentials compared to the respective ReNCP evidence that the oxidation occurs at the macrocycle and peripheral substituents are involved in π conjugation; theoretical calculations also support this [64].

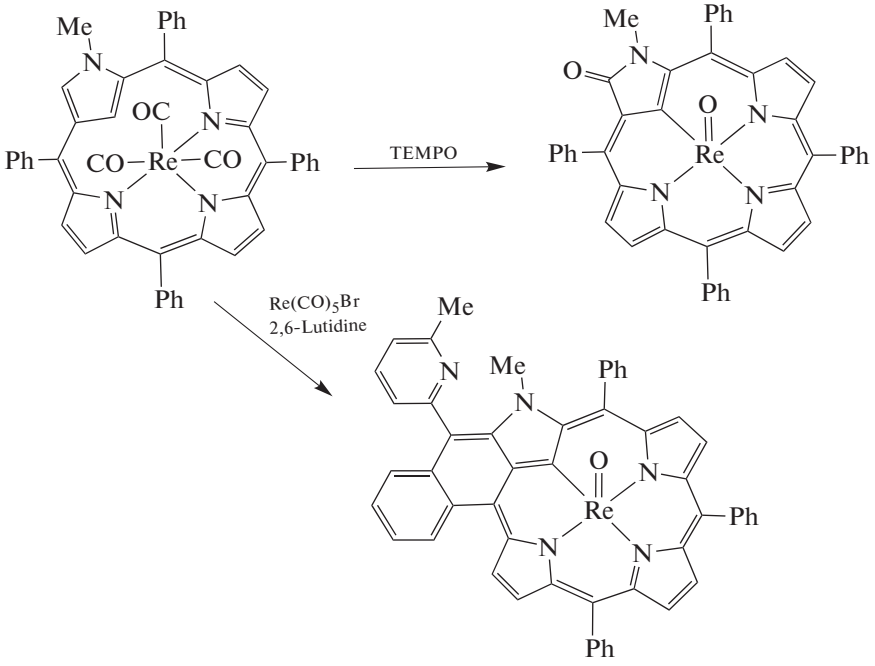

Scheme 1. Chemical oxidation of Re^{I}(NCTPP).

The far higher potentials referring to the oxidation of the macrocycle are shown by unique mono- and dihetero complexes of $Re(CO)_3$ with thiaporphyrin, seleniumporphyrin, and oxaporphyrin, where one or two of the pyrrole rings of the porphyrin are replaced by thiophen, furan, and selenophen, respectively. The relevant potentials are as follows: 1.10 and 1.43 V ($STPPRe^{I}(CO)_3$) (Fig. 4, structure **4**); 1.65 V ($S_2TTPRe^{I}(CO)_3$); 1.15 and 1.74 V ($Se_2TTPRe^{I}(CO)_3$) (Fig. 4, structure **5**); 0.88 and 1.33 V ($OTPPRe^{I}(CO)_3$) (Fig. 4, structure **6**) [65, 66]. Such complexes are highly resistant to oxidation despite the severe distortion of the molecule upon complexation with the Re^{+} ions relative to the parent free macrocyclic base.

The electrochemical behavior of tetrapyrrole rhenium(V) complexes is documented in the literature as data on oxorhenium(V) triarylcorroles (Fig. 5, structure **7**) [67]. The results of redox studies and the values

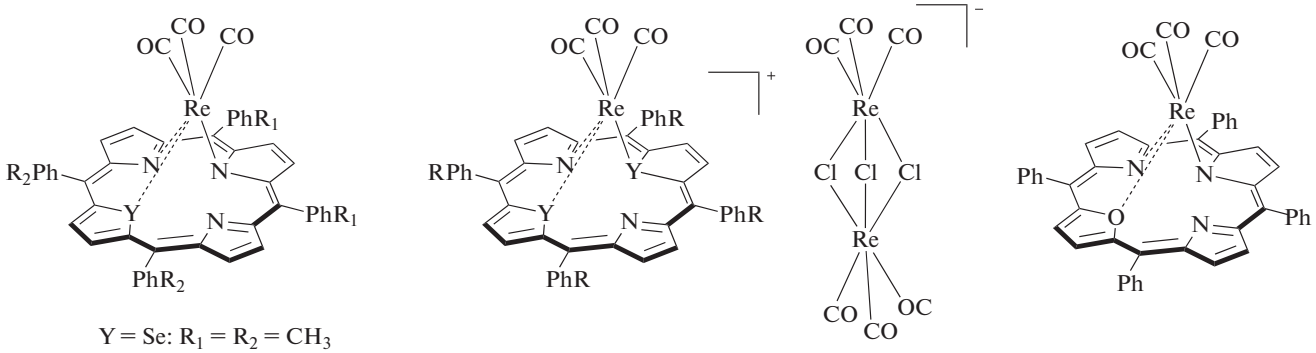

Y = Se: $R_1 = R_2 = CH_3$

Y = S: $R_1 = R_2 = H$; $R_1 = CH_3$, $R_2 = OCH_3$

4 **5** **6**

Structures **4**–**6**

Fig. 4. Chemical structure of heteroporphyrin rhenium complexes (structures **4**–**6**).

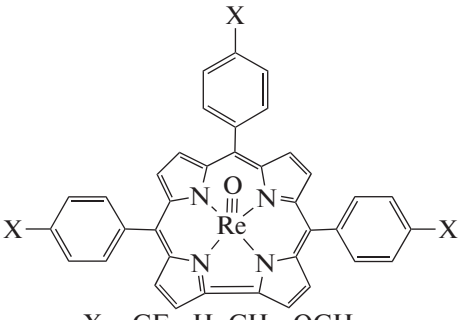

Structure **7**

Fig. 5. Chemical structure of oxorhenium(V)triarylcorroles (structure **7**).

of E_{ox} (0.93–1.10 V) indicate the possibility of macrocyclic oxidation of the compounds.

The cited data show that no one of these rhenium compounds can be oxidized at the central atom upon electrochemical exposure under the conditions studied in the potential range 0–2 V. The Re(I) → Re(V) transition by a chemical route (Scheme 1) is possible for the above-mentioned compound Re^{I}(NCTPP) [64]. The Re(I) → Re(VII) chemical oxidation succeeded in only one case. The preparation of rhenium(VII) trioxo complex $NFPReO_3$ (NFP = *N*-fused porphyrin) via oxidation of the rhenium(I) complex $NFPRe(CO)_3$ using $Me_3NO \cdot 2H_2O$ in 1,2-$Cl_2C_6H_4$ at 140°C for 30 min exemplified the impressive ability of *N*-fused porphyrins to stabilize metal complexes in high oxidation states due to coordination with three nitrogen atoms and a relatively small coordinating cavity (Scheme 2) [68].

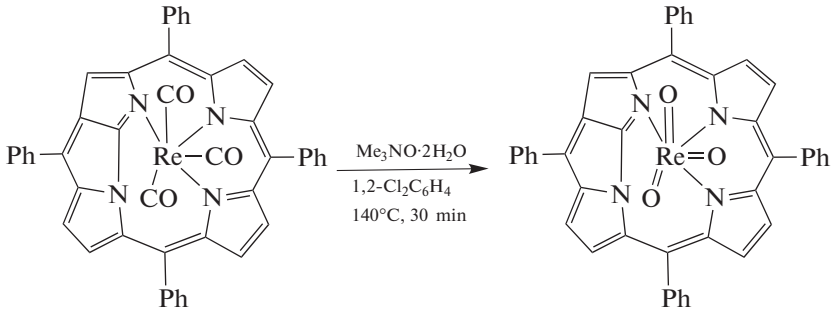

Scheme 2. Chemical oxidation of Re^{I}(NFTPP).

An attempt to prepare a rhenium(VII) complex from the precursor rhenium(V)corrole using an oxidizing agent was unsuccessful, thereby confirming the preliminary theoretical calculations [67].

In general, the reactivity of porphyrin rhenium(V) complexes in solutions is mainly manifested in the exchange of axial ligands [34, 69]. However, rhenium(V) compounds with H_2TPP, H_2OEP, and its *meso*-phenyl-substituted analogues appeared in the group of compounds for which the authors of this survey found and studied the chemical generation of oxidized species in aerated acids (HOAc, H_2SO_4, and CF_3COOH) and in HOAc–H_2SO_4 mixtures (Table 2, [70–73]). One-electron oxidation occurs due to the interaction of the coordination center with molecular O_2 under an excess of protons:

$$(X)_{n-2}\,MP + O_2 + H^+ \rightarrow (X)_{n-2}\,MP^{+\cdot} + HO_2^{\cdot}.$$

The assignment of intermediates and the control of the MP oxidation rate were carried out on the basis of the characteristic UV–Vis spectra of the π-radical cation forms of the MPs. The chemical structures of intermediates and end reaction products were verified, when possible, by additional studies using IR spectroscopy and one- and two-dimensional NMR spectroscopy.

The $O{=}Re^{V}(X)P$ compounds with various coordination sphere compositions in equatorial and axial directions were used as an example to elucidate the effect of the nature of the ligand on the processes that occur in sulfuric acid solutions of the complexes by general Scheme 3 [70–73].

In complexes containing *meso*-phenyl substituents and axial chloride ions in the *cis* position to the oxo ligand, Cl^- substitution by hydrogen sulfate ions is beneficial for removal of an electron from the π system

Table 2. Oxidized forms of selected iridium and rhenium porphyrin complexes in protic solvents

Complex	Solvent (*C*, mol/L)	Species
$[O{=}ReTPP]_2O$	5–10 H_2SO_4/HOAc	$O{=}Re(HSO_4)TPP^{\bullet+}$
O=Re(Cl)OEP	16.78–18.1 H_2SO_4	$O{=}Re(Cl)(O_2)OEP$[a]
O=Re(OPh)OEP	16.8–18.1 H_2SO_4	$O{=}Re(OPh)(O_2)OEP$[a]
O=Re(OPh)MPOEP	16.8–18.2 H_2SO_4	$O{=}Re(OPh)(O_2)MPOEP$[a]
O=Re(Cl)MPOEP	16.8–18.2 H_2SO_4	$O{=}Re(HSO_4)MPOEP^{\bullet+}$
$O{=}Re(Cl)^{5,15}DPOEP$	16.8–18.1 H_2SO_4	$O{=}Re(HSO_4)^{5,15}DPOEP^{\bullet+}$
O=Re(X)P[b]	16.8–18.2 H_2SO_4	$O{=}Re(X)(O_2)P$[a]
$(Cl)(H_2O)IrTPP$	0.043 H_2O/HOAc	$(OAc)(HOAc)IrTPP^{\bullet+}$
	99[c] CF_3COOH	$(CF_3COO)_2Ir^{IV}TPP$
	16.78–18.09 H_2SO_4	$(HSO_4)_2Ir^{IV}TPP^{\bullet+}$

[a]The species stable toward oxidation under given conditions. [b]P = 5,15-bis(4'-methoxyphenyl)-3,7,13,17-tetramethyl-2,8,12,18-tetraethylporphyrin dianion; X = Cl, OPh, or OH. [c]*C*, %.

of the macrocyclic ligand. In O=Re(Cl)OEP, O=Re(OPh)OEP, and O=Re(OPh)MPOEP, and in O=Re(Cl), O=Re(OPh), and O=Re(OH) complexes with 5,15-bis(4'-methoxyphenyl)-3,7,13,17-tetramethyl-2,8,12,18-tetraethylporphyrin, the reaction stops at the stage of formation of a cationic complex with axially coordinated oxygen and the outer-sphere ion (Scheme 3: upper line).

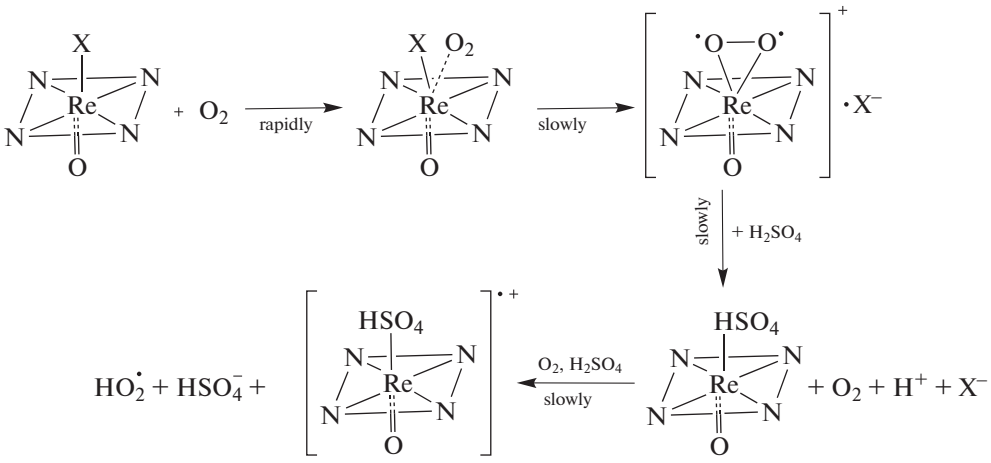

Scheme 3. Chemical oxidation of $O{=}Re^{V}(X)P$ in concentrated H_2SO_4.

An attempt to chemically generate a π-cation radical of μ-oxodimeric $[O = ReTPP]_2O$ under the action of *tert*-butyl hydroperoxide (C = 0.19 mol/L in benzene), monitored by EAS, should have led to a reaction involving the rupture of the μ-oxo-bridge upon coordination of the hydroperoxide molecule with preservation of the coordination center [74]. However, no one of the final equilibrium solute species had a spectrum corresponding to the spectrum of the macrocyclic-oxidized species.

Under an excess of CF_3COOH in CH_2Cl_2 solution, $STTPRe^{I}(CO)_3$), $S_2TTPRe^{I}(CO)_3$), and $Se_2TTPRe^{I}(CO)_3$ heteroporphyrins (structures **4** and **5**) do not form π-radical cations but only undergo protonation at the intracyclic nitrogen atoms. The ^1H NMR titration of compounds using CF_3COOH in $CDCl_3$ showed a low-field shift of pyrrole protons, verifying the occurrence of the process [65, 66]. Rhenium(V) oxaporphyrin (structure **6**) under similar

conditions experiences dissociation to a protonated form of the macrocyclic ligand [66]. The oxidation stability of these compounds is due to their above-mentioned high oxidation potentials.

Axial substitution for ions and molecules of the reaction medium, typical of rhenium complexes, also precedes the generation of highly oxidized iridium(III) porphyrin species in media with high proton concentrations (Table 2) [75, 76]. The location of the unpaired electron during the chemical oxidation of $(Cl)(H_2O)IrTPP$ in acids is dictated by the acidity of the medium and the nature of axial ligands. In 100% AcOH, an aromatically oxidized form of the complex is slowly formed; in CF_3COOH, oxidation of the central metal ion occurs to form an iridium(IV) complex; and in concentrated H_2SO_4, both processes occur in sequence (Scheme 4).

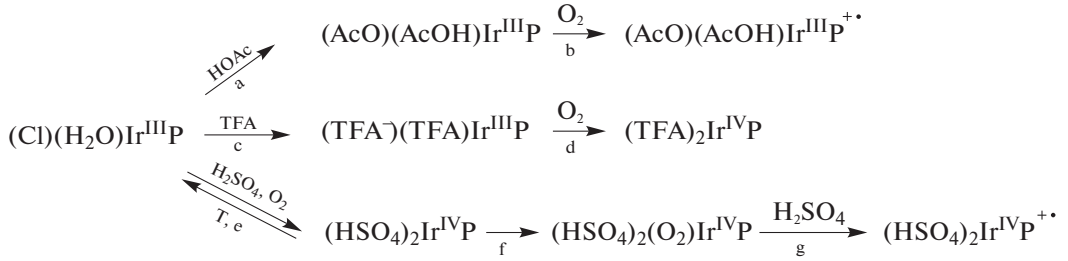

Scheme 4. $(Cl)(H_2O)IrTPP$ transformations in proton-donating solvents.

Coordinated trifluoroacetic acid molecules and anions (Scheme 4, reaction c), having electron-drawing properties, have the cis effect on the coordinated macrocycle and reduce the π-electron density on its atoms, so the iridium(III) complex is not oxidized at the macrocycle (Scheme 4, reaction d). The mixed electron-donor-and-acceptor nature of hydrogen sulfate ions in $(HSO_4)_2Ir^{IV}TPP$, which have both lone electron pairs and energy-accessible vacant *d* orbitals, in combination with the high acidity of sulfuric acid promotes two successive oxidation reactions at the central atom and at the macrocycle (Scheme 4: reactions e and g). The feasibility of the $Ir^{III} \rightarrow Ir^{IV}$ transition is supported by electrochemical studies: the $[(TPP)Ir]^+/[(TPP)Ir]^{2+}$ redox pair has a relatively low $E_{1/2}$ of about 1.4 V [2].

Oxidation at the central metal atom was also observed in the course of the oxidative addition of AcOH to the iridium(I) complex with molecular porphyrin $[IrCl(H_2O)_2]_2H_2TPP$ (SAT complex), a very rare reaction for porphyrin complexes (Scheme 5) [77].

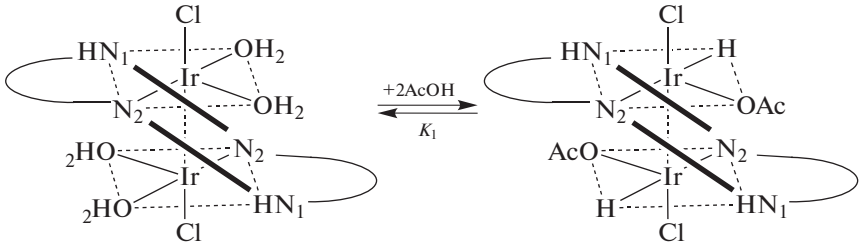

Scheme 5. Oxidative addition of AcOH to $[IrCl(H_2O)_2]_2H_2TPP$.

The electron-donor-and-acceptor nature of oxidizers is likely to be responsible for the differing products formed by the $(Cl)(CO)Ir^{III}TTP$ complex with some oxidizers [78]. The reaction with pyridine-*N*-oxide or trimethylamine-*N*-oxide leads to the coordination of oxidizer molecules in the axial position of the complex to substitute for the chloride ion while not forming oxidation products. Hydrogen peroxide H_2O_2 and *meta*-chloroperbenzoic acid do not react with the test compound, as evidenced by the data of ^1H NMR and mass spectrometry used in the work. It was only in the course of reaction with iodosylbenzene $(PhIO)_n$ that a paramagnetic oxidized complex species was formed, presumably an iridium(V) complex, with the loss of axial CO. However, neither convincing evidence for the formation nor the structure of a high-valence species or intermediate was presented in the study.

For the axial σ complex $Ir(C_8H_{13})TPP$, an option was shown both for chemical oxidation by a one-electron oxidizer $[(4\text{-}BrC_6H_4)_3N](SbCl_6))$ at the axial substituent and for the stabilization of the central cation in an oxidation state >3+ due to the reactions of axial addition and substitution of PPh_3, Cl^-, and

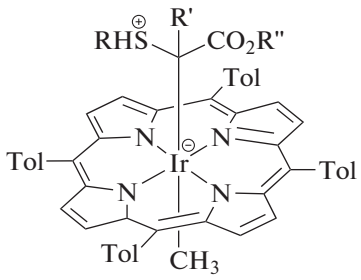

Structure **8**

Fig. 6. Complex intermediate in the reaction of carbene intervention into S–H bonds (structure **8**).

$(L_{OEt})Ru(N)Cl_2$ (L_{OEt} = $(\eta^5\text{-}C_5H_5)Co\{P(O)(OEt)_2\}_3^-$) ligands [79]. The conclusions were supported by electrochemical measurements and X-ray structural analysis.

The above-considered properties of IrP and ReP oxidized species determine the prospects for the practical use of porphyrin complexes of these metals. The high stability of the complexes both in the oxidized and in the reduced states opens up the room for their use not only in catalysis, but also in the design of redox potential switches. Rich redox chemistry can lead in the future to the development of indicators of oxygen optical sensors. An example of water splitting cells with a photoanode based on the porphyrin complex $IrO_2 \cdot nH_2O$ has already been described [80]. The perfor-

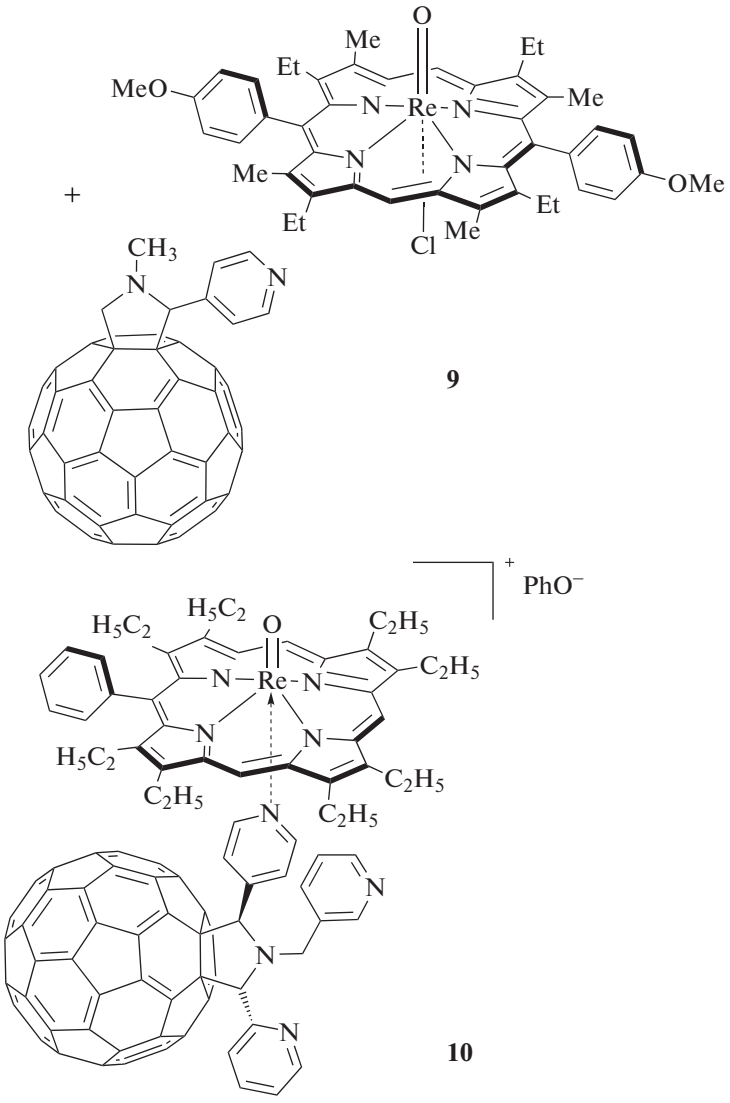

Structures **9** and **10**

Fig. 7. Chemical structure of porphyrin rhenium(V) complexes with monopyridyl-substituted fullero [60]pyrrolidine (stoichiometry unknown, precursors shown) (structure **9**) and tripyridyl-substituted fullero [60]pyrrolidine (structure **10**).

mance of stable redox intermediates of IrP and ReP in the processes they catalyze was noted in many studies. In the (5,10,15,20-tetratolylporphyrinato)methyliridium(III)-catalyzed intervention of carbenes prepared from ethyl-, methyl-, methylphenyl-, and methyl-(*n*-tolyl)diazoacetate, into the S–H bonds of aromatic and aliphatic thiols at the ambient temperature, for example, such the intermediate is the neutral catalyst species with an excessive electron on the iridium (Fig. 6, structure **8**) [21].

Taking into account the high reactivity along the axial axis, we can assume the successful use of the electron–donor properties of IrP and ReP in donor–acceptor coordination pairs with the property of photoinduced electron transport. Two such systems (Fig. 7, structures **9** and **10**) have been prepared and characterized by physicochemical methods in the ground state in our works [34, 81].

CONCLUSIONS

Our brief overview of the work in recent decades concerned with iridium and rhenium complexes with porphyrins and their analogues has shown that the main problem on the way of promoting this topic is the lack of description of specific intermediate forms of complexes in chemical and photophysical transformations. The coordination compounds of these rare metals with substituted, expanded, *N*-fused, *N*-confused, and modified porphyrins, corroles, and heteroatomic macrocycles as well are excellent systems for studying the properties and reactivity at various bonds. The fact that these complexes constitute a special group with remarkable properties is evident from the data presented. They simultaneously exhibit high stability in metal–nitrogen bonds and high reactivity in axial ligand substitution reactions, which, along with rich redox chemistry, makes them promising candidates for use in catalysis. Corrole complexes have been structurally characterized and studied as photosensitizers in photodynamic cancer therapy. While IrP and ReP can perform as excellent electron donors, the photoinduced formation of radical salts in donor–acceptor pairs for organic solar cells remains an almost completely unexplored area.

One who intends to study oxidized species of IrP and ReP is to prepare them under the conditions where they are long-lived. Therefore, methods for generating these species should be developed further. Data on the existence and behavior of oxidized species in various environments and in various reactions will make it possible to model transformations with the catalytic participation of IrP and ReP, to recognize the mechanisms of such transformations, and to extend the list of studied technical processes and biochemical reactions. We hope that the results of this work will help for the better understanding of fundamentals of the chemistry of redox processes involving macrocyclic iridium and rhenium complexes, and will contribute to the development of new complexes with a potential for use in interdisciplinary fields and catalytic research in the future.

ACKNOWLEDGMENTS

The authors used equipment of the Shared Facilities Center of the Upper Volga Regional Center for Physicochemical Research to obtain their own data.

FUNDING

This work was fulfilled in the frame of the Program of State Assignments to the Academy of Sciences (theme no. 0092-2014-0002).

CONFLICT OF INTEREST

The authors declare that they have no conflicts of interest.

REFERENCES

1. K. Koren, R. I. Dmitriev, S. M. Borisov, et al., ChemBioChem **13**, 1184 (2012). https://doi.org/10.1002/cbic.201200083
2. T. L. Lam, T. Ka Chung, C. Yang, et al., Chem. Sci. **10**, 293 (2019). https://doi.org/10.1039/c8sc02920b
3. I. K. Thomassen, L. J. McCormick-McPherson, S. M. Borisov, et al., Sci. Rep. **10**, 7551 (2020). https://doi.org/10.1038/s41598-020-64389-3
4. K. Naoda and A. Osuka, J. Porphyr. Phthalocyanines **18**, 652 (2014). https://doi.org/10.1142/s1088424614500382
5. A. B. Alemayehu, H. Vazquez-Lima, S. J. Teat, et al., ChemistryOpen **8**, 1298 (2019). https://doi.org/10.1002/open.201900271
6. S. M. Borisov, R. F. Einrem, A. B. Alemayehu, et al., Photochem. Photobiol. Sci. **18**, 1166 (2019). https://doi.org/10.1039/c8pp00473k
7. S. Majumder, B. P. Borah, and J. Bhuyan, Dalton Trans. **49**, 8419 (2020). https://doi.org/10.1039/d0dt00813c
8. J. Xie, C. Liang, S. Luo, et al., ACS Appl. Mater. Interfaces **13**, 27934 (2021). https://doi.org/10.1021/acsami.1c06381
9. L. P. Zhang, Y. Geng, L. J. Li, et al., Chem. Sci. **12**, 5918 (2021). https://doi.org/10.1039/d1sc00126d
10. S. Majumder, B. P. Borah, and J. Bhuyan, Dalton Trans. **49**, 8419 (2020). https://doi.org/10.1039/d0dt00813c
11. X. Huang and J. T. Groves, Chem. Rev. **118**, 1021 (2018). https://doi.org/10.1021/acs.chemrev.7b00373
12. C. W. Machan, ACS Catal. **10**, 2640 (2020). https://doi.org/10.1021/acscatal.9b04477
13. G. Passard, D. K. Dogutan, M. Qiu, et al., ACS Catal. **8**, 8671 (2018). https://doi.org/10.1021/acscatal.8b01944

14. T. Lomova, Y. Tsaplev, M. Klyueva, and E. Ovchenkova, J. Organomet. Chem. **945**, 121880 (2021). https://doi.org/10.1016/j.jorganchem.2021.121880
15. J. F. Hartwig, H. M. Key, P. Dydio, et al., US Patent WO 2017/066562 A2 (2017).
16. J.-C. Wang, Z.-J. Xu, Z. Guo, et al., Chem. Commun. **48**, 4299 (2012). https://doi.org/10.1039/C2CC30441D
17. B. J. Anding, A. Ellern, and L. K. Woo, Organometallics **31**, 3628 (2012). https://doi.org/10.1021/om300135f
18. B. J. Anding and L. K. Woo, Organometallics **32**, 2599 (2013). https://doi.org/10.1021/om400098v
19. P. Dydio, H. M. Key, H. Hayashi, et al., J. Am. Chem. Soc. **139**, 1750 (2017). https://doi.org/10.1021/jacs.6b11410
20. Y. Wang, H. Cui, Z.-W. Wei, et al., Chem. Sci. **8**, 775 (2017). https://doi.org/10.1039/c6sc03288e
21. T. O. Dairo and L. K. Woo, Organometallics **36**, 927 (2017). https://doi.org/10.1021/acs.organomet.6b00947
22. W. Yang, H. Zhang, L. Li, et al., Organometallics **35**, 3295 (2016). https://doi.org/10.1021/acs.organomet.6b00490
23. W. P. Shum and H. S. Kesling, US Patent No. 5103027 (1992).
24. J. Buchler, M. Schmidt, and G. Prascher, US Patent No. 4973718 (1990).
25. J. Buchler, S. Kruppa, M. Schmidt, and G. Prascher, US Patent No. 4987226 (1991).
26. J. P. T. Zaragoza, M. A. Siegler, and D. P. Goldberg, Chem. Commun. **52**, 167 (2016). https://doi.org/10.1039/C5CC07956J
27. M. Toganoh, K. Fujino, S. Ikeda, and H. Furuta, Tetrahedron Lett. **49**, 1488 (2008). https://doi.org/10.1016/j.tetlet.2007.12.117
28. T. Yamamoto, M. Toganoh, and H. Furuta, Dalton Trans. **41**, 9154 (2012). https://doi.org/10.1039/c2dt30885a
29. H. X. Wang, K. Wu, and C. M. Che, Synlett **32**, 249 (2021). https://doi.org/10.1055/s-0040-1707221
30. Y. J. Bian, X. Y. Qu, and K. S. Chan, Organometallics **39**, 1376 (2020). https://doi.org/10.1021/acs.organomet.0c00100
31. S. Manas, J. L. P. Armando, and José Armando L. Da Silva, Coord. Chem. Rev. **439**, 213911 (2014). https://doi.org/10.1016/j.ccr.2021.213911
32. A. B. Sorokin, Coord. Chem. Rev. **389**, 141 (2019). https://doi.org/10.1016/j.ccr.2019.03.016
33. M. L. Xiao, J. B. Zhu, G. R. Li, et al., Angew. Chem., Int. Ed. Engl. **58**, 9640 (2019). https://doi.org/10.1002/anie.201905241
34. N. G. Bichan, E. Yu. Tyulyaeva, T. N. Lomova, and A. S. Semeikin, Russ. J. Org. Chem. **50**, 1361 (2014). https://doi.org/10.1134/S1070428014090218
35. D. N. Tritton, G. B. Bodedla, G. L. Tang, et al., J. Mater. Chem. A **8**, 3005 (2020). https://doi.org/10.1039/c9ta12492f
36. T. N. Lomova, Appl. Organomet. Chem. e6254 (2021). https://doi.org/10.1002/aoc.6254
37. T. Tański, P. Jarka, M. Szindler, et al., Appl. Surf. Sci. **491**, 807 (2019). https://doi.org/10.1016/j.apsusc.2019.04.274
38. M. C. R. Castro, N. Ben Sedrine, T. Monteiro, and A. V. Machado, Spectrochim. Acta, Part A **235**, 118309 (2020). https://doi.org/10.1016/j.saa.2020.118309
39. I. Morishima, Y. Takamuki, and Y. Shiro, J. Am. Chem. Soc. **106**, 7666 (1984). https://doi.org/10.1021/ja00337a002
40. D. Dolphin, A. Forman, D. C. Borg, et al., Proc. Natl. Acad. Sci. USA **68**, 614 (1971).
41. N. Carnieri and A. Harriman, Inorg. Chim. Acta **62**, 103 (1982). https://doi.org/10.1016/S0020-1693(00)88485-6
42. T. Satoh, M. Minoura, H. Nakano, et al., Angew. Chem., Int. Ed. Engl. **55**, 2235 (2016). https://doi.org/10.1002/anie.201510734
43. K. Sudoh, T. Satoh, T. Amaya, et al., Chem. Eur. J. **23**, 16364 (2017). https://doi.org/10.1002/chem.201703664
44. M. Mutoh, K. Sudoh, K. Furukawa, et al., Asian J. Org. Chem. **8**, 352 (2019). https://doi.org/10.1002/ajoc.201900085
45. Y. Matano, *Proceedings of the 11th International Conference on Porphyrins and Phthalocyanines*, Buffalo, USA, 2021, p. 145.
46. E. N. Ovchenkova, N. G. Bichan, A. A. Tsaturyan, et al., J. Phys. Chem. C **124**, 4010 (2020). https://doi.org/10.1021/acs.jpcc.9b11661
47. E. T. Shimomura, M. A. Phillippi, H. M. Goff, et al., J. Am. Chem. Soc. **103**, 6778 (1981). https://doi.org/10.1021/ja00412a055
48. M. A. El-Attar, N. Xu, D. Awasabisah, et al., Polyhedron **40**, 105 (2012). https://doi.org/10.1016/j.poly.2012.03.034
49. S. Dey, D. Sil, Y. A. Pandit, and S. P. Rath, Inorg. Chem. **55**, 3229 (2016). https://doi.org/10.1021/acs.inorgchem.5b02065
50. Y. A. Pandit, S. J. Shah, and S. P. Rath, Z. Anorg. Allg. Chem. **644**, 856 (2018). https://doi.org/10.1002/zaac.201800247
51. T. T. H. Tran, Y.-R. Chang, T. K. A. Hoang, et al., J. Phys. Chem. A **120**, 5504 (2016). https://doi.org/10.1021/acs.jpca.6b03538
52. W. R. Scheidt, B. Cheng, K. V. Reddy, and K. E. Brancato, J. Porphyr. Phthalocyanines **21**, 273 (2017). https://doi.org/10.1142/S1088424617500080
53. V. N. Nemykin, S. V. Dudkin, M. Fathi-Rasekh, et al., Inorg. Chem. **54**, 10711 (2015). https://doi.org/10.1021/acs.inorgchem.5b01614
54. D. E. Nevonen, L. S. Ferch, V. Y. Chernii, et al., J. Porphyr. Phthalocyanines **24**, 894 (2020). https://doi.org/10.1142/s1088424619502043
55. F. A. Walker, Inorg. Chem. **42**, 4526 (2003). https://doi.org/10.1021/ic026245p
56. J. Mack and M. J. Stillman, J. Porphyr. Phthalocyanines **5**, 67 (2001).

https://doi.org/10.1002/1099-1409(200101)5:1<67::AID-JPP300>3.0.CO;2-3

57. C. Swistak, J. L. Cornillon, J. E. Anderson, and K. M. Kadish, Organometallics **6**, 2146 (1987). https://doi.org/10.1021/om00153a020
58. J. H. Palmer, T. Brock-Nannestad, A. Mahammed, et al., Angew. Chem., Int. Ed. Engl. **50**, 9433 (2011). https://doi.org/10.1002/anie.201102913
59. J.-L. Cornillon, J. E. Anderson, C. Swistak, and K. M. Kadish, J. Am. Chem. Soc. **108**, 7633 (1986). https://doi.org/10.1021/ja00284a030
60. S. K. Yeung and K. S. Chan, Organometallics **24**, 6426 (2005). https://doi.org/10.1021/om050661a
61. K. M. Kadish, Y. J. Deng, C.-L. Yao, and J. E. Anderson, Organometallics **7**, 1979 (1988). https://doi.org/10.1021/om00099a012
62. K. M. Kadish, D. Schaeper, L. A. Bottomley, et al., J. Inorg. Nucl. Chem. **42**, 469 (1980). https://doi.org/10.1016/0022-1902(80)80030-3
63. K. Murata, Y. Koike, and K. Ishii, Chem. Commun. **56**, 13760 (2020). https://doi.org/10.1039/d0cc04625f
64. T. Yamamoto, M. Toganoh, S. Mori, et al., Chem. Sci. **3**, 3241 (2012). https://doi.org/10.1039/c2sc20708g
65. T. Kaur, W.-Z. Lee, and M. Ravikanth, Inorg. Chem. **55**, 5305 (2016). https://doi.org/10.1021/acs.inorgchem.6b00214
66. A. Ghosh and M. Ravikanth, Inorg. Chem. **51**, 6700 (2012). https://doi.org/10.1021/ic300344g
67. R. F. Einrem, K. J. Gagnon, A. B. Alemayehu, and A. Ghosh, Chem. Eur. J. **22**, 517 (2016). https://doi.org/10.1002/chem.201504307
68. M. Toganoh, S. Ikeda, and H. Furuta, Chem. Commun. 4589 (2005). https://doi.org/10.1039/b508208k
69. J. W. Buchler and S. B. Kruppa, Z. Naturforsch. **45**, 518 (1990).
70. E. Yu. Tyulyaeva, N. G. Bichan, and T. N. Lomova, Russ. J. Inorg. Chem. **58**, 1366 (2013). https://doi.org/10.1134/S0036023613110223
71. N. G. Bichan, E. Yu. Tyulyaeva, and T. N. Lomova, Russ. J. Inorg. Chem. **59**, 1445 (2014). https://doi.org/10.1134/S0036023614120079
72. N. G. Bichan, E. Yu. Tyulyaeva, and T. N. Lomova, Russ. J. Phys. Chem. **88**, 1719 (2014). https://doi.org/10.1134/S0036024414100045
73. N. G. Bichan, E. Yu. Tyulyaeva, T. N. Lomova, and A. S. Semeikin, Russ. J. Inorg. Chem. **62**, 1576 (2017). https://doi.org/10.1134/S0036023617120208
74. O. R. Simonova, S. V. Zaitseva, N. G. Bichan, and E. Yu. Tyulyaeva, *Proceedings of the XIIth All-Russian Conference* "*Solvation and Complexation Problems in Solutions. From Effects in Solutions to New Materials*," Ivanovo, 2015, p. 201.
75. E. Yu. Tyulyaeva, E. G. Mozhzhukchina, N. G. Bichan, and T. N. Lomova, Russ. J. Inorg. Chem. **60**, 157 (2015). https://doi.org/10.1134/S0036023615020199
76. E. Yu. Tyulyaeva, N. G. Bichan, E. G. Mozhzhukchina, and T. N. Lomova, Russ. J. Phys. Chem. **90**, 37 (2016). https://doi.org/10.1134/S0036024416010325
77. T. N. Lomova, *Axially Coordinated Metalloporphyrins in Science and Practice* (Krasand, Moscow, 2018). https://www.rfbr.ru/rffi/ru/books/o_208717
78. L. S. Park-Gehrke, *Doctor of Philosophy Dissertation*, University of Washington, DC, 2010.
79. S.-C. So, W.-M. Cheung, W.-H. Chiu, et al., Dalton Trans. **48**, 8340 (2019). https://doi.org/10.1039/c9dt00244h
80. B. D. Sherman, S. Pillai, G. Kodis, et al., Can. J. Chem. **89**, 152 (2011). https://doi.org/10.1139/V10-118
81. N. G. Bichan, E. N. Ovchenkova, and T. N. Lomova, Russ. J. Phys. Chem. A **93**, 703 (2019). https://doi.org/10.1134/S003602441904006X

Translated by O. Fedorova